CLM-P619

CLM-P619

UKAEA

Preprint

TOPICAL SPECTROSCOPIC FEATURES OF THE EMISSION FROM HIGHLY-IONISED ATOMS IN TOKAMAK DISCHARGES

N. J. PEACOCK

CULHAM LABORATORY
Abingdon Oxfordshire

1980

CLM-P 619

TOPICAL SPECTROSCOPIC FEATURES OF THE EMISSION FROM HIGHLY-IONISED ATOMS IN TOKAMAK DISCHARGES

N J Peacock
Culham Laboratory, Abingdon, Oxon, OX14 3DB, UK
(Euratom/UKAEA Fusion Association)

ABSTRACT

Spectral features from impurity ions in tokamak plasmas are routinely studied in fusion research on account of their influence on the overall energy balance and plasma behaviour. Emission from highly-stripped ions has also a wider significance and topicality in astrophysics and atomic spectroscopy. All of these interests are represented in this discussion of topical problems relating to line emission from the present generations of tokamaks.

The role of charge transfer in tokamaks heated by neutral beam injection is described. This atomic process is observed to lower the effective impurity charge state and increase radiation losses. In the case of completely ionised impurities in the core plasma and at low beam energies $\sim$ 25 keV, as in the DITE tokamak, it is a particularly effective recombination mechanism. Charge exchange from background neutral hydrogen can also be responsible for impaired beam transport and increased radiation loss at the plasma periphery.

The appearance of forbidden lines extending through the X-ray region to the visible is another noteworthy feature of tokamak spectra. The identification and diagnostic use of the M1 and intersystem transitions within the ground configuration of 3- to 9-electron ions of the common metals are discussed.

The importance of 1- and 2-electron spectra in the XUV and X-ray spectral regions is highlighted by the analyses of their resonance lines and associated satellites to derive the electron and ion temperature, ion diffusion and ionisation state of the plasma.

A more fundamental interest is the possibility of using the 1- and 2- electron spectra in tokamaks for measurements of the radiative (QED) energy level shifts and for deriving atomic rate coefficients.

(Paper presented at the 10th Summer School and Symposium on the Physics of Ionised Gases, Dubrovnik, Yugoslavia, 25-29 August, 1980.)

September 1980
cms

important in the case of completely ionised impurities in the core with low beam energies ≤ 25 keV and high beam currents as in the DITE tokamak, Axon et al (1980).

On the topic of forbidden lines, Section 4, recent theoretical analysis and experimental studies, Lawson and Peacock (1980), Lawson et al (1980) have succeeded in identifying many of the (M1) transitions within the ground configuration of 3- to 9-electron systems in the common metals. The diagnostic uses of these lines have been indicated by several authors e.g. Suckewer and Hinnov (1978), Feldman, Doschek et al (1980).

Emission from highly-stripped ions in tokamaks has of course a wider significance in astrophysics and in atomic spectroscopy. All of these interests are represented in a consideration of the line emission from 1- and 2-electron systems in the present generation of tokamaks as discussed in Section 5. Model calculations, e.g. Gabriel (1972), Bhalla et al (1975), of the intensities of the satellites to the allowed resonance lines of H-like and He-like ions were originally constructed to interpret solar plasmas. Since these features are also prominent in the x-ray spectrum of keV temperature tokamaks, Bitter, Hill et al (1979), the model calculations may be tested in the well diagnosed conditions of tokamak plasmas, Bitter, Von Goeler et al (1979). Line intensity ratios such as the intercombination relative to the allowed lines in 2-electron ions can be related to the ground state population of adjacent ion stages and departure of the populations from their predicted stationary values in tokamaks can be interpreted in terms of ion diffusion, Peacock and Summers (1978).

Of more fundamental interest is the possibility of using the keV temperature plasmas in tokamaks not only for measurements of the atomic rate coefficients but also of the radiative (QED) energy level shifts in the 1- and 2-electron ions. This last topic is also discussed in Section 5.

2. CHARGE TRANSFER RECOMBINATION

Collisions between atoms and ions in which the ion picks up one or more of the atomic electrons,

$$A^{q+} + B \rightarrow A^{(q-1)+} + B^{+} \quad (1)$$

has been recognised since the 1920's. Much of the past research on charge transfer has been concerned with the transport of energetic, often highly-ionised ions through neutral gas or thin solid films and has been reviewed by Betz (1972). Theoretical treatments of the electron exchange has been reviewed by Bransden (1972).

1. INTRODUCTION

Spectral features from impurity ions in tokamak plasmas are routinely studied in fusion research on account of their influence on the overall energy balance and plasma behaviour. The concentration of highly charged ions of the common metals, e.g. Fe, and light gases, e.g. O, can be sufficiently high as to radiate away a major fraction of the heat input Jensen et al (1977), whether this be by ohmic heating e.g. Hugill et al (1977) or by high energy neutral particle injection e.g. Suckewer, Hinnov et al (1980). The spatial concentration of impurities and their charge state depends on particle diffusion coupled with the ionising and recombination rates. Impurity ion transport in tokamaks is in itself a complex problem, Stringer (1977), Samain and Werkoff (1977), in comparison with which the atomic collision processes, Summers and McWhirter (1979) Wiese (1978) may be judged to be relatively straightforward. The impurities through the local effective ion charge, $Z_{eff} = \sum_i \frac{n_i Z_i^2}{n_e}$, can alter the electrical current distribution within the torus and therefore change the plasma stability.

Tokamak plasmas, in terms of their operating density $\sim 5 \times 10^{12} \leq n_e \leq 5 \times 10^{14}$ cm^{-3} and temperature $\hat{T}_e \gtrsim 1$ keV, occupy a unique place in laboratory plasmas. The impurity ions in the core of the plasma have characteristically a high ionisation potential $\psi_i \simeq$ several keV while the relative population of their ionic species is approximately coronal. The low collision rates $\sim 10^3 \rightarrow 10^5$ sec^{-1} ensure that forbidden lines, extending from the x-ray region to the visible, are noteworthy features of the tokamak emission spectra. The plasma is often sufficiently well behaved and reproduceable to contemplate the evaluation of atomic collision rates from spectral line intensities, Breton et al (1978). Recently interest has focused on the charge transfer process which is observed to lower Z_{eff} and increase the radiation loss in the core plasma of tokamak experiments with H^o beam injection, Afrosimov et al (1978), Hulse et al (1980), Suckewer, Hinnov et al (1980). Charge exchange from background thermal H^o can also be responsible for impaired beam transport and increased radiation loss at the plasma periphery. This topic, treated in Section 2, is particularly

However, little of this early work has been concerned with the interaction between energetic neutral beams of light atoms, e.g. H^o, with highly ionised ion species viz,

$$Z^{q+} + H^o \rightarrow Z^{(q-1)+} + H^+ \quad , \qquad (2)$$

a common enough situation in present day tokamaks. In calculating the charge exchange cross-section, only the relative interaction velocity, V_r, of the particles is important. For beam velocities $V_n(H^o) >> V_{th}(Z^{+q})$ the thermal velocity of the impurity ions, we need make no distinction between V_r and V_n for beam injection experiments into plasmas of fusion interest.

A unified theory of the 3-body charge-transfer interaction, applicable over a wide range of incident particle energies and involving discrete quantum states of the donor atoms and acceptor ion is prohibitively difficult. However, various theoretical models have been used, their validity depending on the atomic structure of the particles and on the magnitude of V_n relative to the hydrogen ground-state orbital velocity, v_o. $v_o = e^2/\hbar = 2.188 \times 10^8$ cm sec^{-1} which is equivalent to a relative interaction energy of 23.3 keV/AMU for impacting particles. These models include the distorted wave approximation, Ryufuku and Watanabe (1978, 1979 a, b) the absorbing sphere model, Olson and Salop (1976) valid for $V_n < 2 \times 10^8$ cm sec^{-1}, the tunnelling model, Gorzdanov and Janev (1978) and the classical trajectory approximation Olson and Salop (1977) the latter being valid for $V_n > v_o$.

A first approximation to the charge exchange cross-section can be derived, however, from the classical treatment of Bohr and Lindhard (1954). The classical approach is reasonable since the de Broglie wavelengths, $\lambda\!\!\!^{-} = \frac{\hbar}{Mv_n}$, of the projectile is much smaller than the collision diameter for the exchange interaction. Using the Bohr Lindhard model, the captive cross-section at low impacting velocities and for highly-charged states, is given by

$$\sigma_1 = \pi R_r^2 = \pi a_o^2 \, q\left(\frac{a}{a_o}\right)\left(\frac{v}{v_o}\right)^{-2} \simeq 10^{-16} \, q \ \text{cm}^2 \qquad (3)$$

in the case where the orbital velocity of the electron equals v_o. In equation (3), $a_o = \frac{\hbar^2}{me^2}$ is the Bohr radius and the "release radius" for the transfer electron is given by

$$\frac{q\ e^2}{R_r^2} = \frac{m\ v^2}{a} \qquad (4)$$

For slow particles and high q therefore the cross-section is independent of the relative interaction velocity of the particle, V_r and is linearly proportional to the charge state of the ion.

At high velocities when $V_r > v_o$, the probability of electron capture is $\left(\frac{v}{a}\right)\left(\frac{R_c}{V_r}\right)$, where the "capture radius" R_c is given by

$$\frac{q\ e^2}{R_c} = \tfrac{1}{2}\ m\ V_r^{\ 2} \tag{5}$$

The cross section for fast particles is then,

$$\sigma_2 = \pi\ R_c^{\ 2}\left(\frac{v}{a}\right)\left(\frac{R_c}{V_r}\right)$$

$$= 8\pi\ a_o^{\ 2}\ q^3\left(\frac{a}{a_o}\right)^{-1}\left(\frac{v}{v_o}\right)\left(\frac{V_r}{v_o}\right)^{-7} \tag{6}$$

and the capture cross-section falls off rapidly with beam velocity, scaling as $q^3 V_r^{\ -7}$. An implicit assumption in this model is that quantum effects can be ignored, i.e. that there is a quasi-continuum of electron states into which the electron can be attached. This is generally true for $q \gtrsim 4$.

In practice the theoretical and experimental data appear to fit reasonably well along universal curves of σ_c/q^k when plotted against $E(\text{keV/AMU})/q^{\ell}$, with $k \simeq 1.0$ and $\ell \simeq 0.5$.

Figure 1 illustrates the magnitude and the shape of the capture cross-section for a typical reaction, $O^{6+} + H^o \rightarrow O^{5+} + H^+$, as a function of the relative velocity of the particles, Crandall (1979). The main results of the Bohr-Lindhard model i.e. constant value of $\sigma_{ch.ex.}$ for $V_r < 2 \times 10^8 \text{cm sec}^{-1}$ and its rapid decrease for $V_r > 2 \times 10^8 \text{cm sec}^{-1}$ are to be noted. At very low velocities, $V_r \sim 10^7$ cm sec^{-1}, theoretical models require consideration of quasi-molecular formation and collision-induced transitions while at very high impacting velocities, $V_r \gtrsim 10^9 \text{cm sec}^{-1}$, ionisation becomes the dominant process.

The magnitude of charge transfer as a recombination process in plasma relative to capture of the free electrons, i.e. collisional dielectronic recombination, e.g. Summers (1974), is illustrated in Fig. 2. The charge exchange coefficient at $V_r \sim v_o \sim \overline{v}_e$ (the thermal velocity of the plasma electrons at T_e = 27.25 eV), is four orders of magnitude higher than the free electron recombination coefficient. At the higher electron temperatures typical

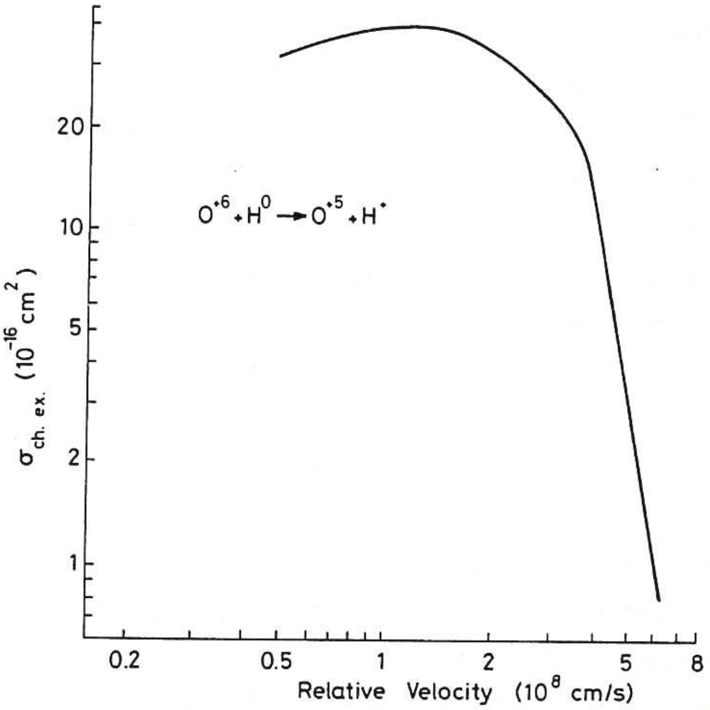

FIG. 1

Charge exchange cross-section for $O^{+6} + H^O \rightarrow O^{+5} + H^+$ as a function of the relative interaction velocity of the particles, Crandall (1979).

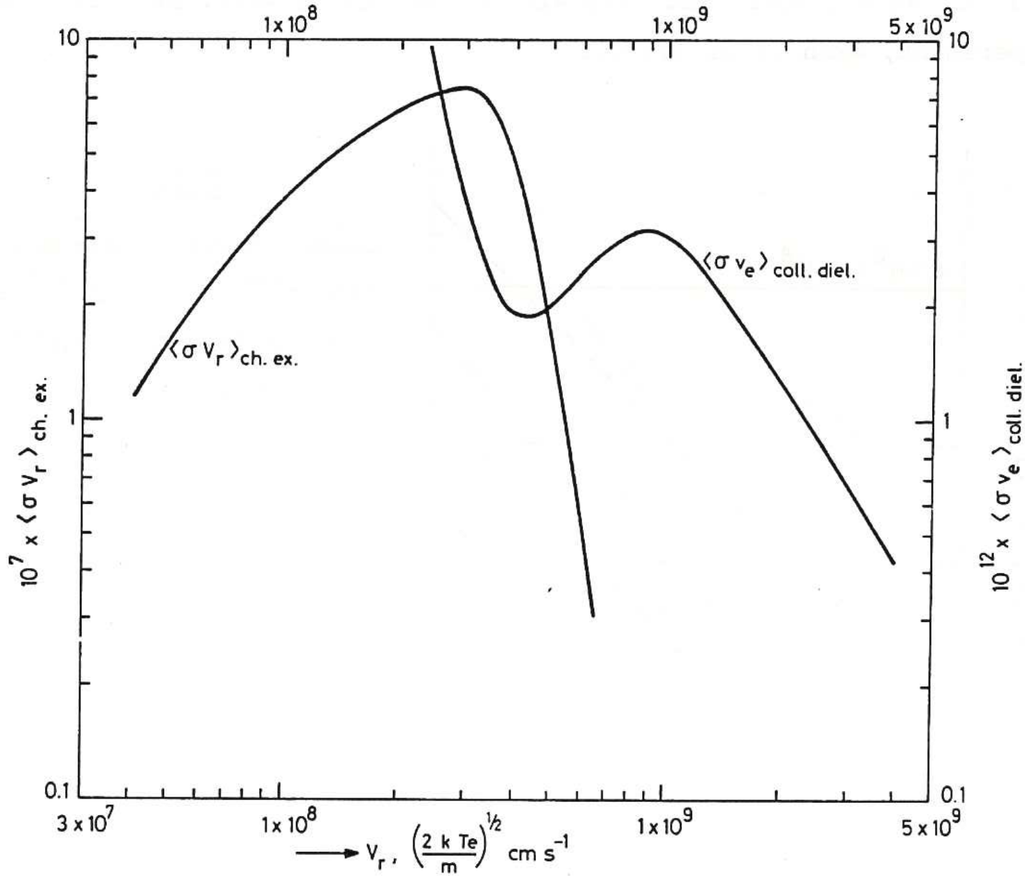

FIG. 2 *Recombination rate coefficients for $O^{6+} \rightarrow O^{5+}$. $\langle \sigma V_r \rangle_{ch.ex.}$ is the coefficient for charge exchange $O^{6+} + H^O \rightarrow O^{5+} + H^+$ as a function of the interaction velocity V_r; $\langle \sigma v_e \rangle_{coll.diel.}$ is the collisional dielectronic rate, Summers (1974), for $n_e = 10^{12} cm^{-3}$ as a function of the most probable electron velocity.*

of tokamak plasmas and for higher ion charge states than $q = 6$, the difference in the coefficients can easily be an order of magnitude greater, $\sim 10^5/_1$. The charge exchange rate $N(H^o)\langle\sigma v\rangle_{ch.ex.}$ is, of course, independent of electron density whereas the total free electron recombination rate $n_e\left[\langle\sigma v\rangle_{rad} + \langle\sigma v\rangle_{diel}\right.$ which is the sum of the collisional-radiative and dielectronic rates, increases linearly with electron density, n_e. Charge transfer is therefore only likely to be a competitive or dominant recombination process when the neutral atoms concentration is

$$N(H^o) \gtrsim 10^{-5}\, n_e \qquad (7)$$

In beam-heated tokamaks, for example with electron parameters and an H^o injection energy of 20 keV/AMU as indicated in Fig. 3, charge transfer recombination of Fe^{+24} ions implies $N(H^o) \gtrsim 10^8 cm^{-3}$. This concentration is fairly typical of the hot thermal neutrals in the core plasma of tokamak devices and it is well exceeded by the concentrations of cold neutrals at the plasma edge and of the energetic neutrals within the beam itself: see, for example, the DITE experiment, Axon et al (1980).

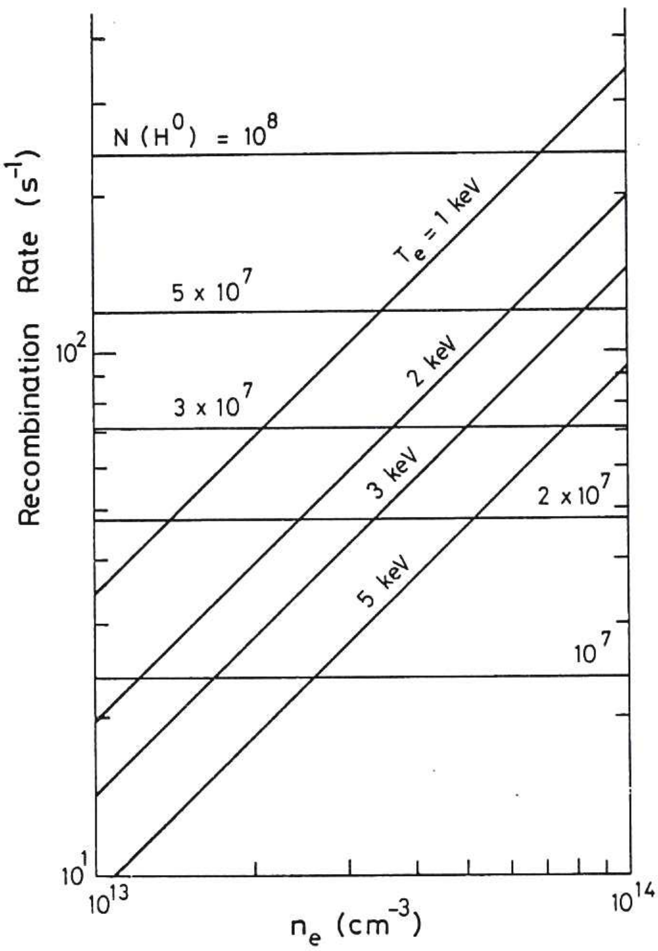

FIG. 3

Charge transfer recombination rate for $Fe^{24+} + H^o \rightarrow Fe^{23+} + H^+$ for various densities $N(H^o)$ of 20 keV/AMU hydrogen neutrals compared with collisional dielectronic rate as a function of electron density: Hulse et al (1980).

3. EFFECTS OF CHARGE TRANSFER ON IONISATION BALANCE AND RADIATION LOSS

The degree of ionisation of the impurities in tokamaks is determined by the ion diffusion rates relative to the atomic rate processes and, in the absence of neutral particles, is given by

$$\frac{\partial N(z^{+q})}{\partial t} = \frac{1}{r}\frac{\partial(r\Gamma_{z,q})}{\partial r} + n_e\left\{\alpha(z^{+(q-1)})N(z^{+(q-1)}) + \beta(z^{+(q+1)})N(z^{+(q+1)}) - \left[\alpha(z^{+q}) + \beta(z^{+q})\right]N(z^{+q})\right\} \qquad (8)$$

where α and β are the ionisation and recombination rates and

$$\Gamma_{z,q} = D\frac{\partial N(z^{+q})}{\partial r} = r\,V_{z,q}\frac{\partial N(z^{+q})}{\partial r}$$

In well-confined plasmas, the diffusion velocities are small enough, $\lesssim 10^3$ cm sec^{-1}, to produce no great departure from the steady-state coronal conditions of ionisation and recombination such as described by Summers (1974), Post et al (1977). The collisional-dielectronic rate computed by Summers (1974) is the appropriate recombination process.

When neutral atoms are present, charge transfer to the impurities represents an additional recombination process the inclusion of which leads to a revised ionisation balance equation, viz.

$$\frac{N(z^{+(q-1)})}{N(z^{+q})} = \frac{\beta_r(z^{+q}) + \beta_{diel}(z^{+q}) + \xi.\beta(z^{+q})}{\alpha(z^{+(q-1)})} \qquad (9)$$

where $\xi = \frac{N(H_o)}{n_e}$, and the RHS is the ratio of the total, collisional-dielectronic plus charge transfer recombination rate to the total electron impact ionisation rate, including inner-shell effects.

A result of the charge exchange term is to decrease the effective charge state on the ions at a given plasma temperature, as illustrated for ionised iron in Fig. 4. In some circumstances the radiation loss is considerably increased and the overall power-balance altered by the inclusion of charge transfer recombination, Krupin et al (1979), Hulse et al (1980). The effect on the radiation loss is greatest when the plasma temperature has a value such that the dominant steady-state, impurity ion species has 1 or 2 electrons. For iron this temperature lies between about 2 keV and 10 keV as

FIG. 4

Iron ion abundances in coronal equilibrium (top) and with additional charge transfer recombination from 20 keV/AMU H^0 neutrals with a concentration $N(H^0)$ = 2×10^8 cm^{-3}. (After Hulse et al (1980)).

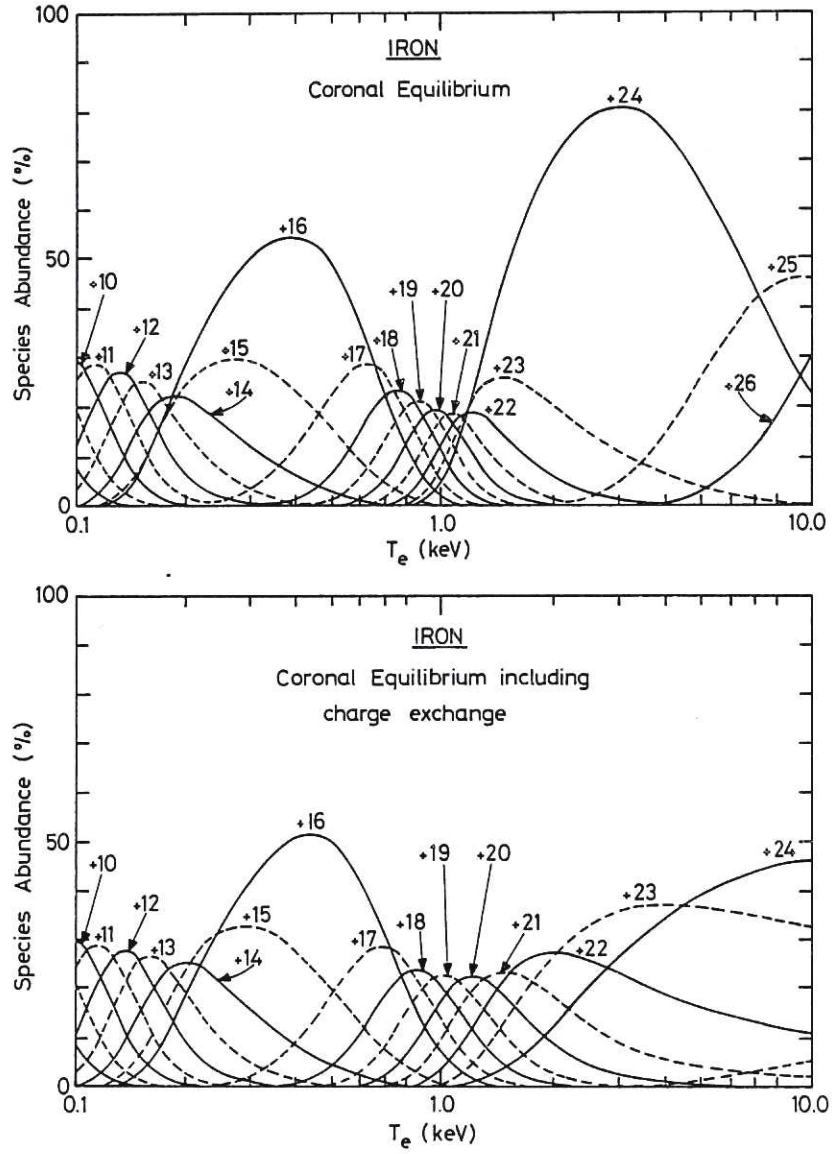

illustrated in Fig. 5. One or two electron configurations persist over a wide range of temperatures, Fig. 4, and are typical of the impurity ion species to be found in the well confined core plasma in tokamaks. The fractional increase in radiation due to charge transfer and its effect on energy confinement can be most dramatic therefore in localised plasma regions.

Experimental evidence for charge transfer recombination in tokamaks has come recently from spectroscopic studies of the time-evolution of the emissivities of different ion species during H^0 injection into PLT, Suckewer et al (1980). A decrease in the emission from the dominant ionisation species, e.g. Fe^{+24} in the core of the PLT plasma, with a concomitant rise in the emissivity of Fe^{23+} during neutral injection, is ascribed to charge transfer recombination. The possibility of alternative explanations such as beam-induced instability mixing of the high temperature core plasma with cooler outer layers, or injection

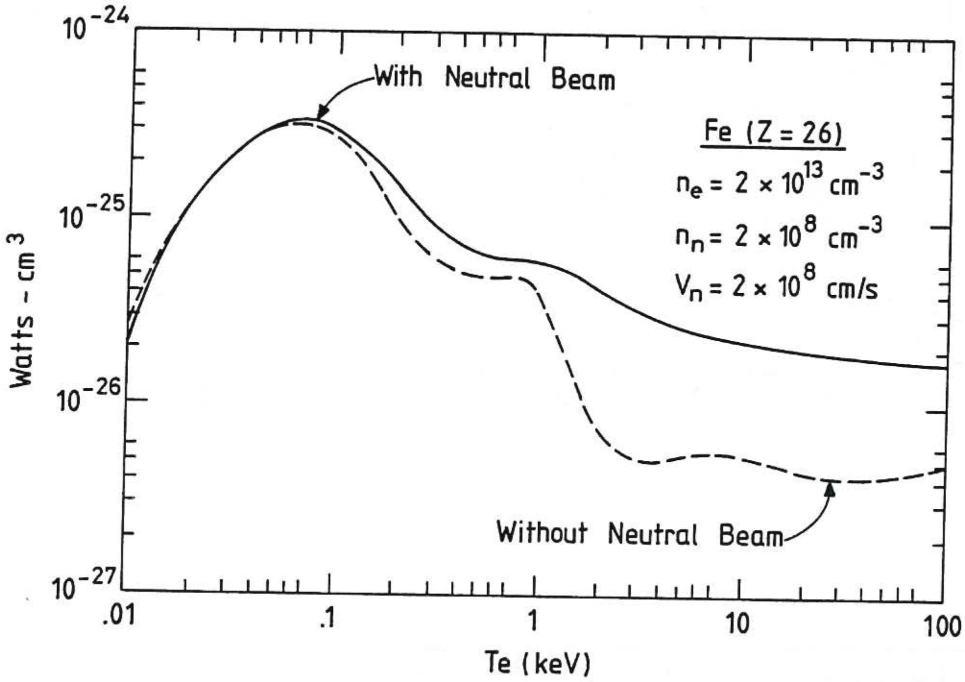

FIG. 5 *Radiation loss per Fe impurity ion from a hydrogen plasma with $n_e = 2 \times 10^{13}$ cm^{-3}, - - - - ; compared with radiation loss with H^O injection, the beam velocity V_n = 2×10^8 cm s^{-1} and the H^O concentration $n_n = 2 \times 10^8$ cm^{-3} ———: Hulse et al (1980).*

of lowly ionised Fe within the H^O beam, is discounted because of the observed increase in T_e during the injection pulse, Fig. 6. Suckewer, Hinnov et al (1980) note that the observed variation in the emissivities, Fig.6, is not due to the charge transfer process *per se* but to the lowering of the effective charge state of the impurities.

Temporal variation of the level populations of the target ions during charge transfer constitutes a more positive piece of evidence for this recombination process. Theoretically, capture into the separate quantum levels is estimated to maximise, Ryufuku and Wantanabe (1978, 1979, a, b), at a principal quantum level of

$$\bar{n} = q^{0.774} \qquad (10)$$

For O^{+8} ions, for example, recombination takes place preferentially into the $\bar{n} = 5$ quantum level. Clearly for recombination to be 'stabilised' by radiative decay then $\bar{n}$ must be less than the so called collision limit n_c, at

FIG. 6

Time evolution of Fe XXIV, Fe XXV, Fe XXII line intensities during neutral D^{o} beam injection into the PLT tokamak. The lower curve shows the temporal variation of the core electron parameters and the rate of charge exchange between D^{o} and Fe XXV: Suckewer, Hinnov et al (1980).

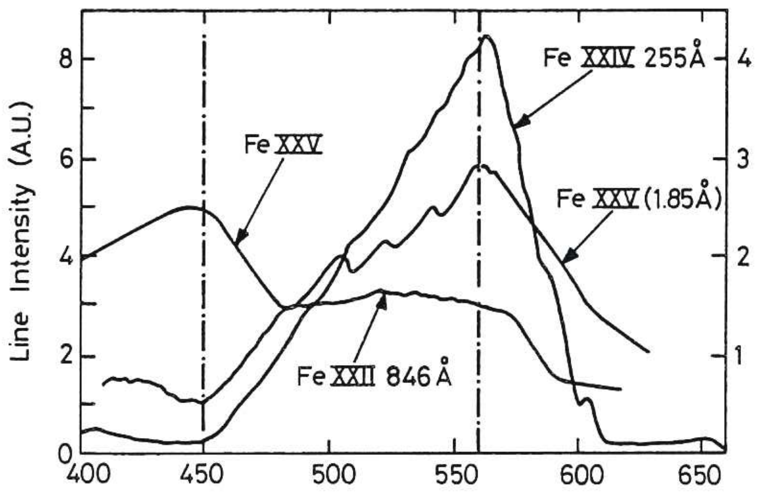

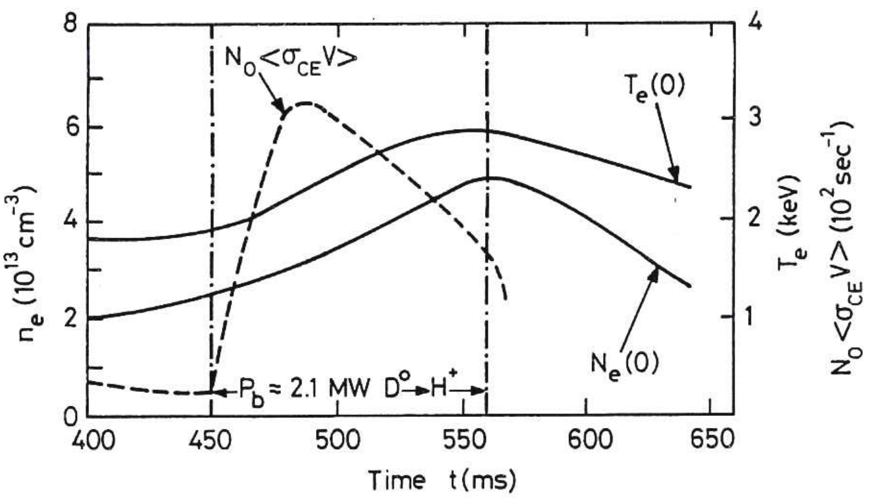

which collisional de-excitation is 10 x radiative decay, a criterion that can be expressed as

$$n_e \gtrsim 1.73 \times 10^{14} \, T_e^{1/2} \, \psi^3(n_c, n_c - 1) \qquad (11)$$

where $\psi(n_c, n_c-1)$ is the excitation potential between n_c and its neighbouring level. For hydrogen ions $\psi(n_c, n_c-1) \simeq \frac{2z^2 Ry}{n_c}$. In tokamak plasmas $\bar{n} < n_c$ is generally the case.

Isler (1977) was among the first to study level population changes during beam injection into tokamaks. The anomalously rapid increase in O^{+7} Balmer-α at 120.36, .51Å during the beam heating pulse in the ORMAK tokamak has been interpreted by Isler (1977) as due to $H^{o} + O^{+8} \rightarrow H^{+} + (O^{+7})^{*}$. The relatively slow increase exhibited by O^{7+} Lyman series can be accounted for by electronic excitation which dominates the emissivities of these resonance lines. It is more difficult to account for the equally slow increase in O^{7+}, Balmer-β, which should, like its Balmer-α counterpart, also show the instantaneous effect of charge-exchange preferentially into the n=5 levels. However, the detailed balance of populating and de-populating processes vary with the angular momentum quantum states (charge exchange occurs preferentially into high azimuthal states) so that temporal emission from Lyman and Balmer lines may indeed differ during beam injection. Clearly, calculations of the detailed atomic state populations are required.

A neat application of charge transfer recombination to the measurement of impurity concentrations have been demonstrated by Afrosimov et al (1978). Using a short period, 0.2m sec, modulated H^{o} beam whose current is sufficiently low not to alter the electron parameters in the plasma, Afrosimov et al (1978) were able to interpret the absolute intensity of C^{+5} Lyman-α in terms of the concentration, $N(C^{+6}) \simeq 10^{11}$ cm^{-3}, of carbon nuclei in the core of the plasma. This 'remote sounding' technique promises to be particularly valuable for estimating the temporal and spatial concentrations of these ions, such as bare nuclei, which do not register their presence by line emission.

The importance of charge transfer processes involving thermal (1→100 eV) neutrals at the plasma edge should not be neglected. Apart from inhibiting beam transport, charge transfer recombination may need to be included in the analysis of spectroscopic features, particularly those discussed by Peacock and Summers (1978) and Brau et al (1980) which are aimed at deriving diffusion rates. Isler and Crume (1978) suggest that intensity anomalies in oxygen lines at 115.8Å and 81.9Å in the ISX-A tokamak are due to preferential population of the n = $4^{2}P$ levels of O^{5+} and the n = 5, ^{3}P levels of O^{6+} by charge exchange from the background thermal H^{o} atoms. All other observed oxygen lines can be accounted for adequately by straightforward electronic excitation.

4. FORBIDDEN LINES IN TOKAMAKS

Since their early identification in the solar corona, Edlen (1945), interest in forbidden lines of highly-ionised atoms has, until recently, been confined to astrophysical plasmas. Magnetic dipole and spin forbidden transitions between levels in the ground configuration and between those and other Δn = 0 excited configurations of $3s^{k}\ 3p^{\ell}$, Behring et al (1976) and $2s^{k}\ 2p^{\ell}$, Doschek et al (1975) are of particular interest since they lie in the visible and VUV regions of the spectrum.

In tokamak plasmas, the parameters are somewhat similar to those of active solar regions so that forbidden lines in these laboratory plasmas now attract considerable attention both theoretically, see Cowan (1977), Doschek and Feldman (1976), Feldman et al (1980) and experimentally, see Suckewer and Hinnov (1978), Suckewer, Fonck and Hinnov (1980) and Lawson, Peacock and Stamp (1980).

Many of the semi-empirical predictions of the forbidden line wavelength involving $2s^k\ 2p^\ell$ configurations have come from the work of Edlen (1969) (1972) (1979 a, b) (1980). The experimental data, summarised by Fawcett (1975) (1978), has been culled from both solar and laboratory sources. For example, information connecting the ground state levels of Fe XX with its excited $\Delta n=0$ configurations, Fig.7 comes from such diverse sources as tokamaks, solar flares and laser-produced plasmas, the last being particularly useful sources for isoelectronic studies of allowed and intersystem lines. From such data together with other published results, complete listings of the $2s^k 2p^\ell \rightarrow 2s^{k-1} 2p^{\ell+1}$ transitions in Li-like to F-like ions of the common metals are now available, Lawson and Peacock (1980).

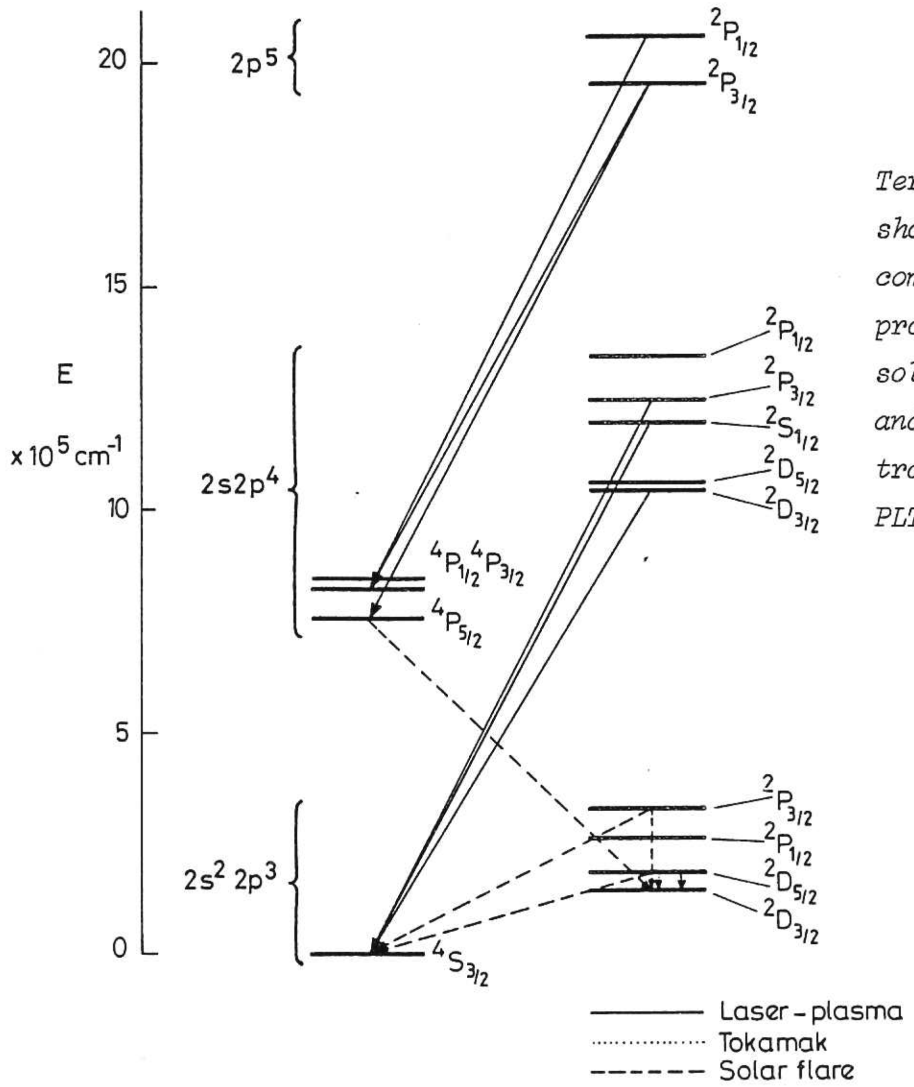

FIG.7

Term scheme of Fe XX showing observed inter-combination lines in laser-produced plasmas ———, solar flare data - - - - and the $^2D_{5/2} - {}_{3/2}$ transition observed in the PLT tokamak.

The spontaneous decay rates of various allowed and forbidden transitions are compared in Fig.8 with the collisional rates typical of tokamak plasma conditions. The dominance of the collisional rates over the A_{ij} values of forbidden lines at low transition energies would lead us to expect, on simple-minded considerations, that only these forbidden lines with $A_{ij} \gtrsim 10^4 sec^{-1}$ and transition energies $\varepsilon \lesssim 10$ eV would be present in the tokamak spectrum.

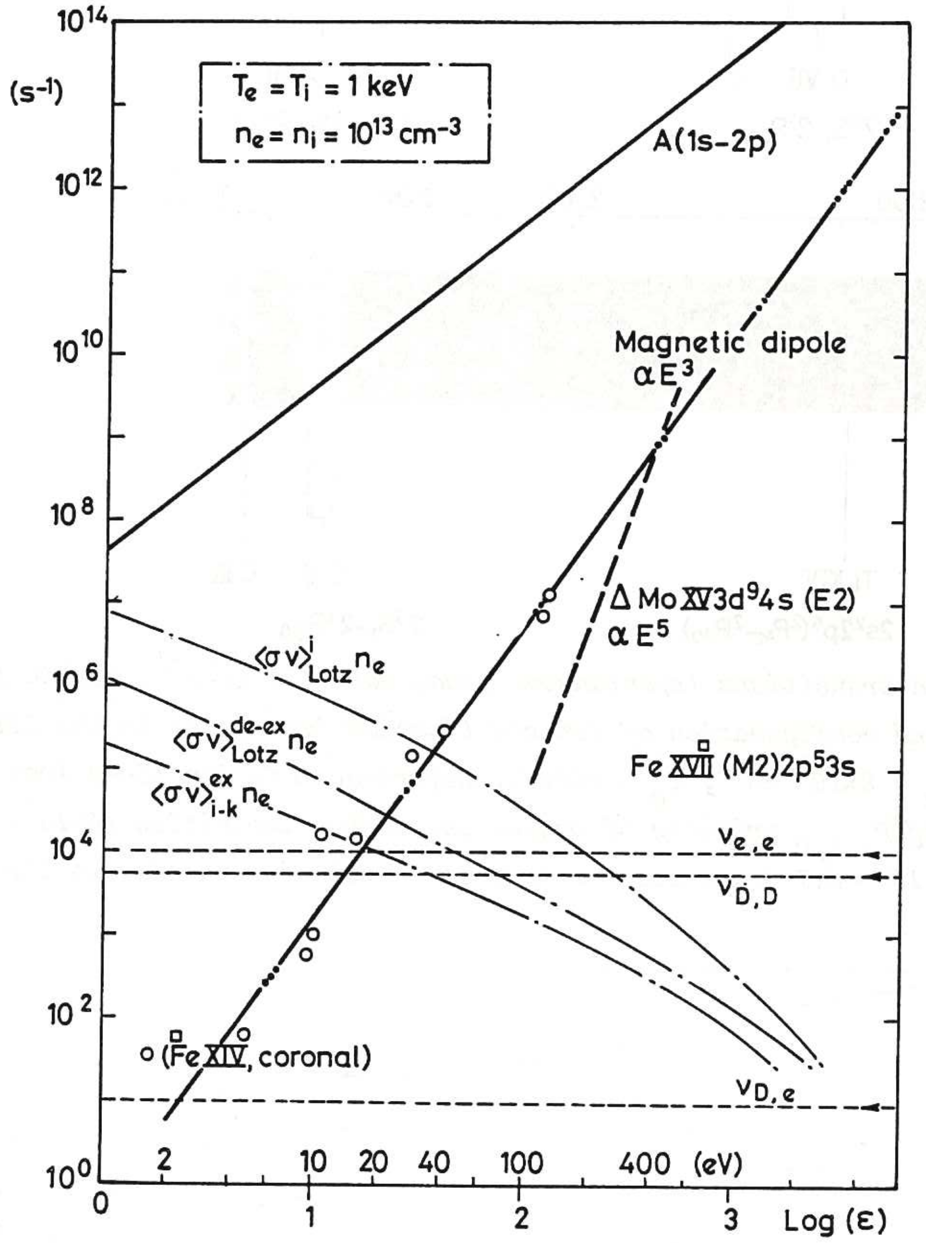

FIG.8 *Spontaneous decay rates for various types of transitions (-.. allowed 1s-2p: -o- magnetic dipole, □ magnetic quadrupole, -Δ- electric quadrupole) versus the transition energy* ϵ*(eV). The collisional decay rates* $\langle\sigma v\rangle n_e$ *(Lotz, 1967) and thermalisation rates* ν_{ee}, $\nu_{D,e}$ *and* $\nu_{D,D}$ *for typical tokamak conditions are plotted for comparison.*

However, even lower energy transitions, particularly those within the $2s^k2p^\ell$ ground configurations of ionised metals have been observed recently in tokamaks and studied by Suckewer and Hinnov (1978), Suckewer, Fonck and Hinnov (1980),

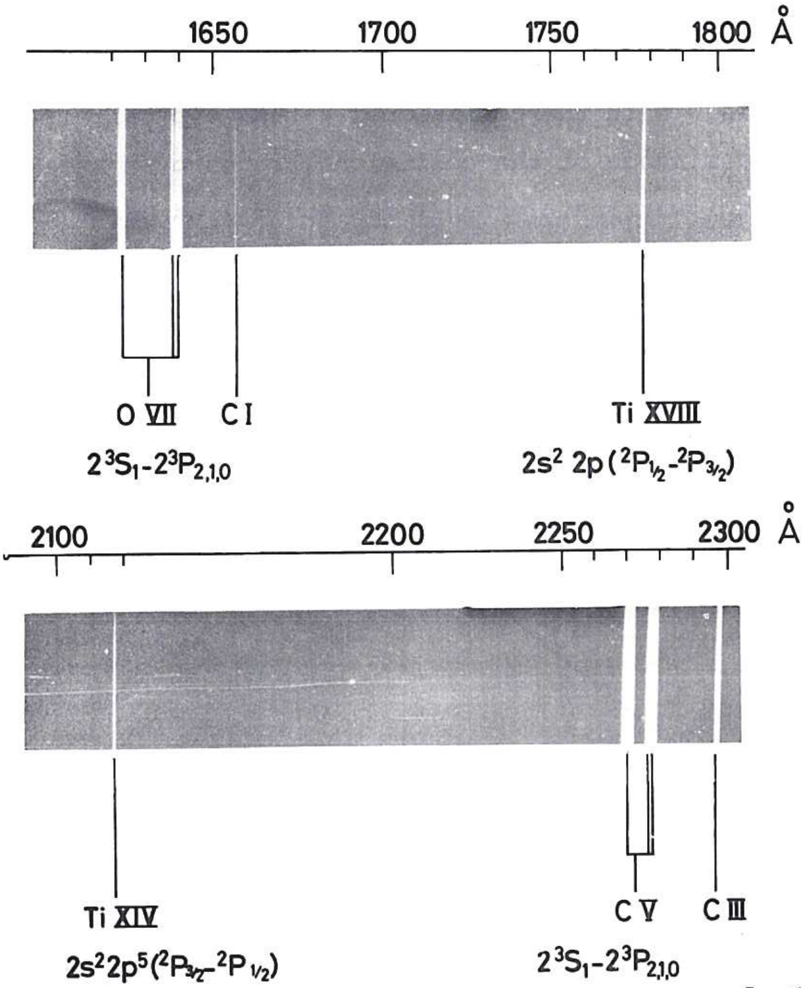

FIG. 9 Forbidden transitions (spontaneous decay rate $A \sim 10^3 s^{-1}$) within the $1s^22p^n$ ground configuration of ionised titanium impurities in the DITE tokamak ($n_e \simeq 2 \times 10^{13} cm^{-3}$, $T_e \sim 800eV$). Reference emission lines from the $1s2s\,^3S_1-1s2p\,^3P_{2,1,0}$ triplets of oxygen and carbon impurities ($A \sim 10^8 s^{-1}$ and $N(0) \sim 10 \times N(Ti)$) are seen to have comparable intensities to the metal lines.

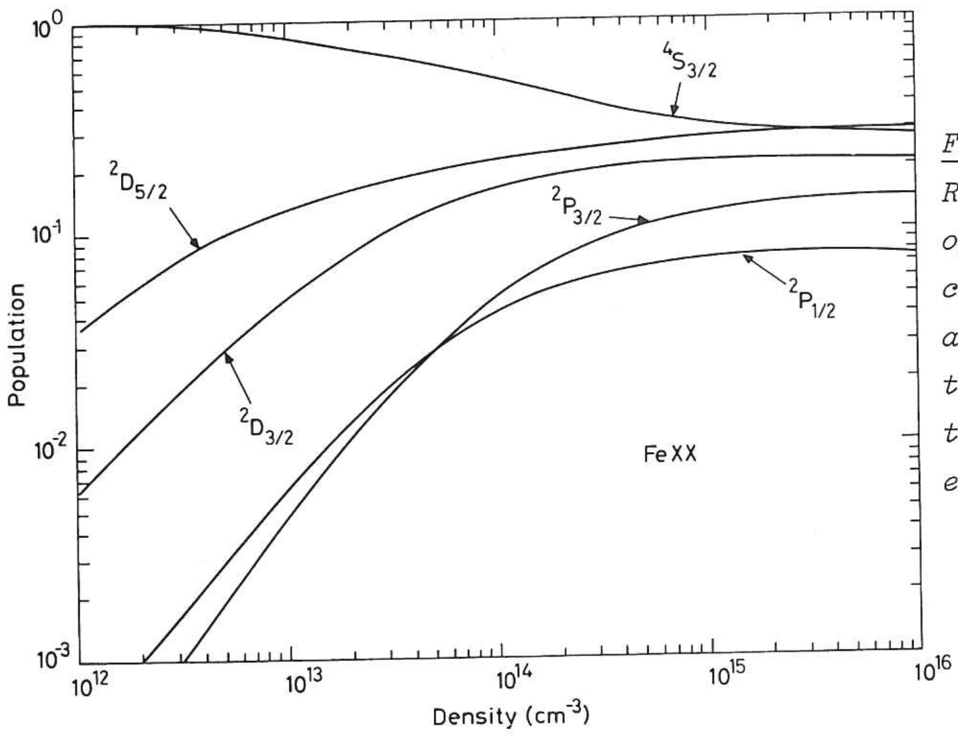

FIG. 10 Relative population of levels in ground configuration of Fe XX at a temperature where this ion species is in the majority, Feldman et al (1980).

Lawson, Peacock and Stamp (1980). The emission intensities of lines with A_{ij} values as low as $10^2 \rightarrow 10^4 sec^{-1}$, can be seen by inspection of the Ti XIV, Ti XVIII emission from the DITE tokamak in Fig.9. Since these $\Delta n=0$ forbidden lines lie at long wavelengths, in the VUV and visible typically, their line profiles are useful monitors of the ion temperature, Eubank et al (1978) and of plasma rotation, Suckewer, Eubank et al (1979). Both of these measurements on the PLT tokamak make use of the $2s^2 2p^3$, $^2D_{5/2-3/2}$ transition in Fe XX at 2665.1Å. Perhaps the most useful information from such lines, however, is impurity ion concentrations which may readily be derived from their absolute intensities. The absolute populations of the ground levels of Fe XX are shown in Fig.10 as a function of electron density. The almost constant populations of these $2s^k 2p^\ell$ levels at $n_e \gtrsim 10^{14} cm^{-3}$, relative to the levels in the excited configurations $2s^{k-1} 2p^{\ell-1}$ which in general increase linearly with n_e, indicate why the long-wavelength forbidden lines are prominent features only of low density high temperature laboratory plasmas such as tokamaks. Feldman et al (1980), Bhatia and Mason (1980), Mason et al (1979) and Doschek and Feldman (1976) have outlined additional diagnostics applications of the forbidden and allowed $n=2 \rightarrow 2$ transitions for measuring T_e and n_e in tokamak plasmas. The intensity ratio of the Fe XX 2665Å forbidden line to the $2s2p^4\ ^4P_{5/2}$ - $2s^2 2p^3\ ^4S_{3/2}$ resonance line at 132.85Å, for example, would be a reasonable monitor of electron density.

The plots in Fig.8 suggest that forbidden lines which lie at wavelengths less than a few hundred angstroms should readily be observed in tokamaks. Apart from intersystem lines of the configurations $2s^2 2p^k \rightarrow 2s2p^{k+1}$ which for the common metals lie typically in the region 80Å→200Å, these shorter wavelength forbidden lines involve changes in total quantum number i.e. $\Delta n>0$. An example is the (E2) resonance decay of the 3d4s(J=2) levels in the first excited configuration of Ni-like MoXV, Fig.11. These transitions, lying at 58.833Å and 57.920Å and with A_{ij} value $\sim 10^7 sec^{-1}$, appear as the strongest line features in the XUV spectrum of the DITE tokamak when operated with a current-limiter of molybdenum, Mansfield et al (1978).

The first excited configuration of neon-like Fe XVII also gives rise to a forbidden (M2) transition, Fig. 12, which is observed at 17.08Å in the solar spectrum and in tokamaks. The $3p^5 3s\ ^3P_2$ transition to the ground state has been observed both in DITE and in the solar spectrum but not in higher density laboratory plasmas. In contrast, the other allowed components such as $3p^5 3s\ ^3P_1$, $^1P_1$ are strong features of almost all Fe plasmas including laser-produced plasmas at temperatures of the order of $T_e \sim 0.5$ keV. It is of

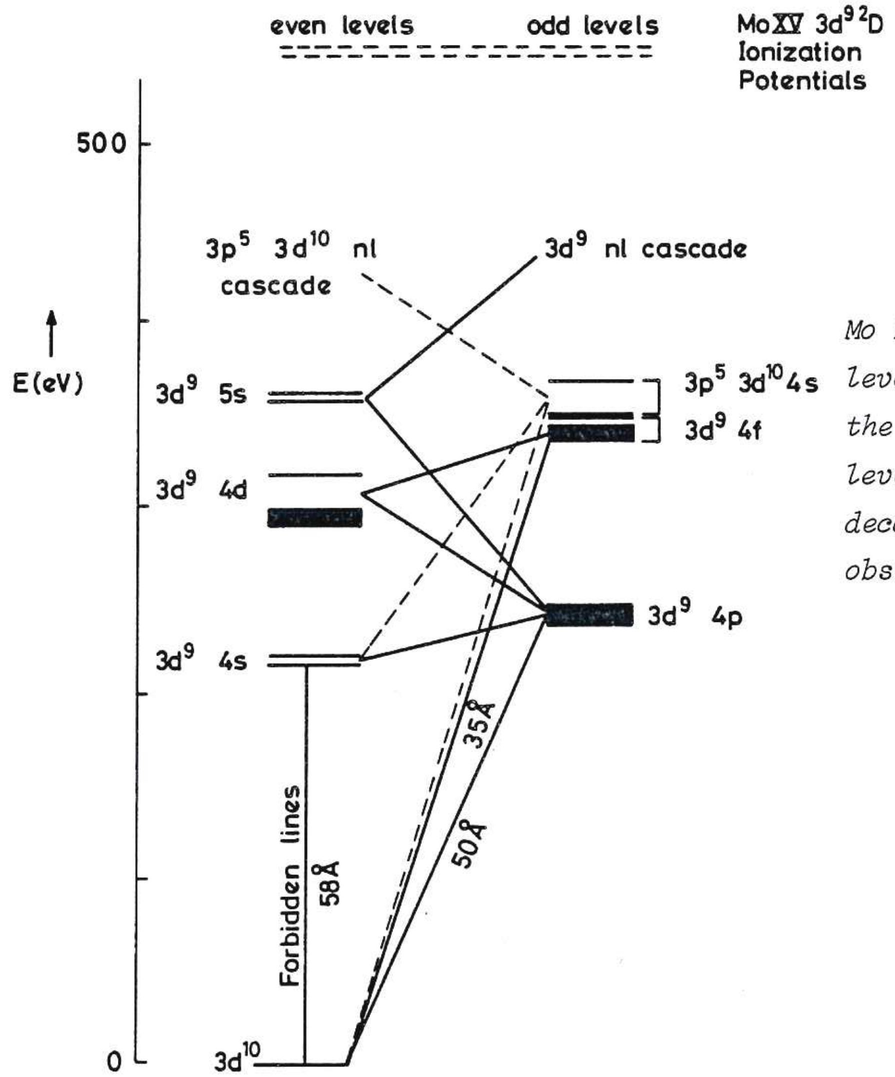

FIG.11

Mo XV (Ni-like) energy level diagram showing the $4d^9 4s$ metastable levels and (E2) resonance decay at 58.833Å and 57.920Å observed on the DITE tokamak.

interest that the relative intensities of all the multiplet components involving resonance decay from $2p^5(^2P)3d,3s$ are insensitive to T_e and n_e, Loulergue and Nussbaumer (1973) and are remarkedly similar in the sun and in the DITE tokamak, Fig.12.

5. 1- and 2-ELECTRON IONS IN TOKAMAKS

Line spectra from H- and He-like ions of impurities is of particular interest on account of the persistently high relative population of these ions over an extended range of temperature, Fig. 4. Below an electron temperature of 1 keV, typical 1- and 2-electron ion species in tokamaks belong to the light elements such as C N O F which may be present to the extent of about 1% or more of the electron density. Above 1 keV the common metals, Ti Cr Fe Ni being representative elements, are often present with concentrations an order of magnitude or so smaller than the lighter impurities.

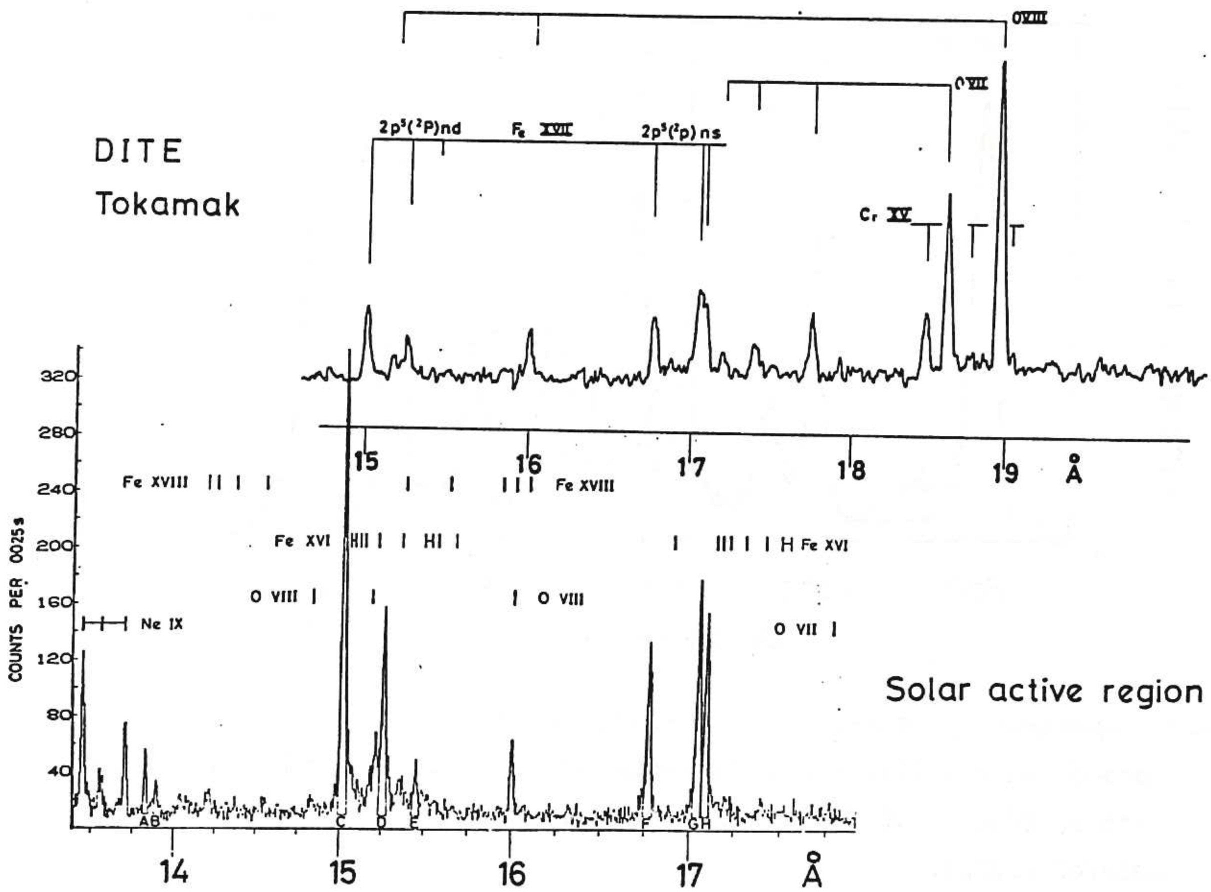

FIG.12 Comparison of soft x-ray spectrum from solar active region and the DITE tokamak showing the main OVIII (Lyman) and Fe XVII $2p^5(^2P)3d,3s$ line features. The $3p^5 3s\ ^3P_2$ (M2) resonance transition at 17.08Å is resolvable in both sources.

5.1 Satellite Line Intensities

The resonance line spectra of 1- and 2-electron ions are accompanied at slightly longer wavelengths by partially-screened 'satellite' transitions of the type

$$1s^p n\ell - 1s^{p-1} n\ell, n'\ell' \qquad (12)$$

with p = 1 or 2.

In the case of He-like ions these transitions are interspersed with the forbidden intersystem lines, viz. the relativistically induced (M1) $1s^2\ ^1S_o$ - $1s2s\ ^3S_1$ and the (M2) $1s^2\ ^1S_o - 1s2p\ ^3P_1$ decay. An example of the line structure on the long wavelength side of the Fe XXV $1s^2\ ^1S_o - 1s2p\ ^1P_1$ allowed resonance line, marked 'w' is shown in Fig. 13. This high dispersion crystal spectrum of the PLT tokamak, Bitter, Hill et al (1979), is of sufficiently high quality to permit detailed comparison of the line shapes and intensities with theory. The features 'x', 'y', 'z', Fig.13 are the intersystem lines arising from the resonance decay of the levels $1s2p\ ^3P_{2,0}$ and $1s2s\ ^3S_1$ respectively, the feature

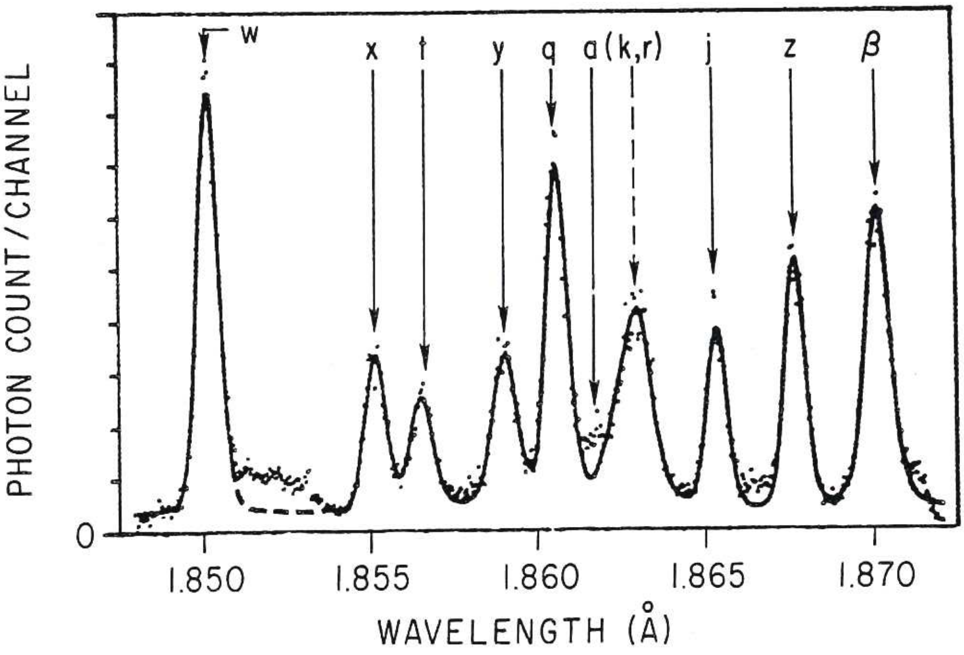

FIG.13 Spectrum of Fe XXV $1s^2\ ^1S_0 - 1s2p\ ^1P_1$ allowed line 'w' and its associated satellites and forbidden lines emitted from the PLT tokamak, Bitter, Hill et al (1979). The line annotation is that ascribed by Gabriel (1972).

'β' is the Fe XXIII Be-like satellite $1s^2 2s^2\ ^1S_0 - 1s2s^2 2p\ ^1P_1$, while the other annotated lines correspond to the Fe XXIV satellites. These Li-like ion transitions are of the type $1s^2 n\ell$ - $1s2pn\ell$ and their intensities have been modelled extensively by Gabriel(1972) and by Bhalla et al (1975). The contribution of higher series numbers with $n \geq 3$ has also been considered by Bely-Dubau et al (1979a, b) and is required to account for the energy in the long wavelength wing of the allowed line 'w' in Fig.13. Finally the effect of non-Maxwellian distributions of the electrons on the overall intensity pattern of these Li-like ion satellites has been considered by Gabriel and Phillips (1980). While the impetus for these model calculations has been the interpretations of solar emission the calculations are also applicable to tokamak plasmas. Indeed, because the laboratory plasmas are well diagnosed and controllable a comparison between the tokamak emission and the model calculations provides a sensitive test to the theory, Bitter, Hill et al (1979): Bitter, Von Goeler et al (1979).

Confining our attention to the Li-ion satellites, these multiply-excited levels can be populated by direct inner-shell excitation of the Li-ion and/or by dielectronic recombination from the He-like ion,

$$e + X^{+(z-2)} \Leftrightarrow X^{+(z-3)}[n'\ell{+}1:n''\ell] \qquad (13)$$
$$\Rightarrow X^{+(z-3)}[n\ell:n''\ell''] + h\nu$$

dielectronic capture of the electron being followed by a stabilising radiative decay with emission of a photon rather than the reverse process of autoionisation. The main contributions come from n' = 2,3 and 6 > n" > 3, so that satellites tend to cluster around the first few members of the allowed resonance series. Provided the doubly-excited level is an autoionising level with the $1s^2 + e$ continuum, the recombination process and the dielectronic satellite intensity is then temperature dependent. The ratio of the dielectronic satellite to the allowed 'w' line, Bely-Dubau et al (1979), is given by

$$\frac{I_s}{I} = \frac{\sqrt{3}}{2} \frac{m\pi a_o^2}{h} \frac{1}{\bar{f}P} \frac{E_o}{kT_e} \frac{g_s}{g_1} \frac{A_R A_a \exp^{[(E_o-E_s)/kT_e]}}{(A_a + \Sigma A_r)} = F_1(T_e)F_2(S) \quad (14)$$

where $F_1(T_e)$ is a function only of T_e and E_o and E_s, the energies of the He-like resonance and Li-like satellite levels above the He-like ion ground state, with statistical weights g_1 and g_s: $F_2(S) = \frac{g_s A_r A_a}{(A_a+\Sigma A_r)}$ is a function only of the autoionising A_a and radiative A_r decay rates: P is a Gaunt factor ~ 0.2 and $\bar{f} \sim 0.6$ is the effective oscillator strength of the allowed line. Such a line is 'j', i.e., $1s^2 2p\ ^2P^0_{3/2} - 1s2p^2\ ^2D_{5/2}$, in Fig.13 and has been used by Bitter, Hill et al (1979) to derive T_e, Fig.14. Other Li-like ion satellites e.g. $1s2p^2\ ^2P^e$, i.e. 'a' of Fig.13, which, neglecting configuration interaction effects, cannot couple by autoionising transitions with the continuum for reasons of parity and angular momentum, can only be present by inner-shell excitation. The most intense of these inner-shell excited satellites of Fe XXIV is $1s^2 2s\ ^2S_{1/2} - 1s2p2s(^1P)\ ^2P^o_{3/2}$ i.e. line 'q' in Fig.13. The relative intensities of lines 'w', 'q', 'β' are proportional mainly to the respective ion populations N(Fe XXV): N(Fe XXIV): N(Fe XXIII), since their upper excited levels have almost the same energy above their ground states. These electron impact excited lines define the equilibrium state of ionisation with a characteristic temperature $T_z = f[N(z)/N(z-1)]$. Comparison of T_z with T_e gives the thermodynamic state of the plasma. Sufficient discrepancy between T_z and T_e has been noted by Bitter, Hill et al (1979) Fig. 14 to throw doubt either on assumptions of coronal ionisation balance in tokamaks or on the rate coefficients used in the model calculations.

The diagnostic potential of the group of lines shown in Fig.13 is not yet exhausted. The broadening of the allowed line 'w' has been interpreted in terms of the ion thermal notion, after due care is taken to subtract the energy in the long-wavelength wing, Fig.13, due to higher series member satellites, Bitter, Von Goeler et al (1979). The relative intensities of the intercombination lines, 'x', 'y' and 'z' are mainly density dependent beyond a threshhold density, and in the case of the PLT tokamak Bitter, Hill et al (1979) satisfactory agreement is found with the theory of Freeman et al (1971).

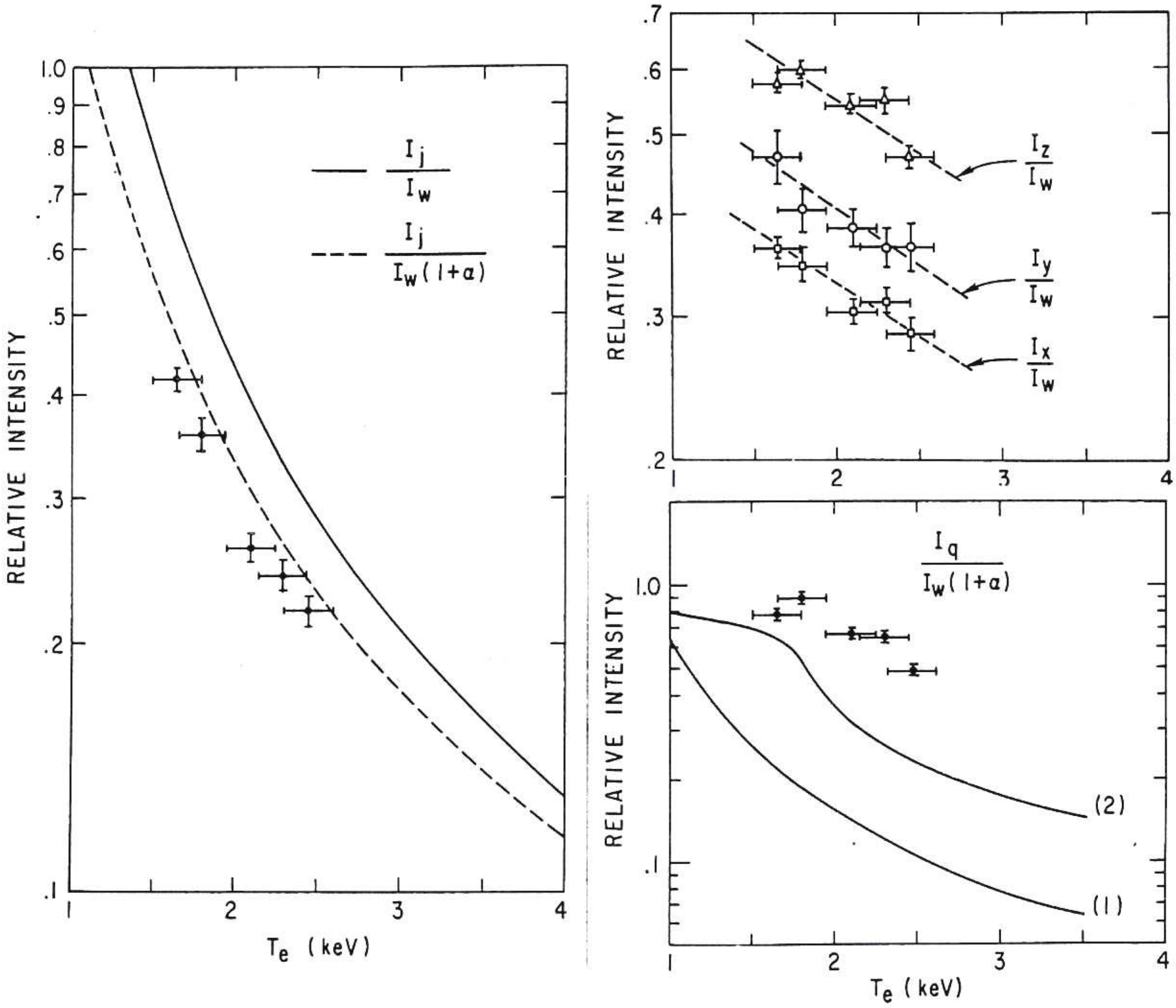

FIG. 14 Analysis of the line intensities of the Fe XXV $1s^2\ {}^1S_0 - 1s2p\ {}^1P_1$ line 'w' and its associated n = 1→2 lines shown in Fig.13. The ratio of 'w' to other line features is fitted to model calculations (see text). The intensity I_j (left) is a dielectronic satellite from the $1s2p^2\ {}^2D_{5/2}$ level from which T_e may be derived, $I_{x,y,z}$ are $1s2p\ {}^3P,\ {}^3S$ level decays (upper right) and I_q (lower right) is the decay from the inner shell excited level $1s2p2s\ {}^2P^0_{3/2}$, its ratio with 'w' being mainly a function of $N(Fe^{23+})/N(Fe^{24+})$. The full lines (lower right) are based on coronal balance calculations: Bitter, Hill et al (1979).

5.2 Recombination Spectrum from 1- and 2-Electron Ions

The total recombination rate of free electrons with impurity ions which are fully stripped or have 1- or 2-electron configurations, is small relative to other ion species. Impurity nuclei are special cases since the dielectronic recombination process for these ions is not possible. Even for 1- and 2-electron systems, the dielectronic rate Burgess (1965), Merts et al (1976) is still small on account of the large excitation energy of the k-electrons. Ion species with L- and M-shell configurations on the other hand have large dielectronic rates which, for intermediate values of Z at least, much exceed the collisional radiative recombination rates. The ionisation rates, Summers (1974) normalised to the temperature at which a particular species is in the majority is also lower for the more highly stripped ions. An immediate consequence of the relative magnitude of these rates arises from the equation of radial ion transport, eq(8), and this is the propensity of nuclei and 1- and 2-electron ions to diffuse further through the plasma without change of valency. The H- and He-like ions therefore occupy a wider plasma radius than do the less highly charged ions.

On some theoretical models the ions are expected to diffuse preferentially inwards towards the hot plasma core. In most tokamak experiments however, accumulation of impurities is not observed and a nearly steady-state local impurity concentration is reached after the initial transient diffusion of ions from the walls and current limiter. The outwards diffusion of the 1- and 2-electron systems to the cooler peripheral plasma, balanced by the inward ion flux, causes several spectral features which are important indicators of the magnitude of the diffusion rates. Firstly, the recombination continuum intensity per ion, with $\langle\sigma v\rangle_{rec.} \propto T_e^{-3/2}$, shows an enhancement at larger plasma radii. Radiative capture of the free electrons by H-like argon seeded into the PLT tokamak, Von Goeler (1979), gives rise to steps in the x-ray recombination as illustrated in Fig.15. These steps, occuring at 4.12 keV the ionisation potential of Ar XVII, are most pronounced at the larger radii where the temperature $T_e \simeq 0.5$ keV, indicating departures from ionisation balance for the Ar^{+17} ion in this plasma region. The extent of this departure is interpreted by Brau et al (1980) in terms of an outwards diffusion rate, which from eq(8) can be expressed as

$$\frac{1}{r}\frac{\partial(r^2 V_{18,17})}{\partial r}\frac{\partial N(Ar^{+17})}{\partial r} = - n_e N(Ar^{+17})\ \beta(Ar^{+17}) \qquad (15)$$

where all the other coefficients for Ar^{+17}, apart from the radiative recombination terms, are negligible at $T_e \simeq 0.5$ keV and $n_e \simeq 2 \times 10^{13}$ cm^{-3}. Diffusion velocities $V_{18,17} \sim 10^3$ cm s^{-1} are derived for the PLT tokamak from eq(15), Brau et al (1980).

Another manifestation of the outwards diffusion of 1-electron systems in tokamaks is the 'anomalous' appearance of the intercombination lines of He-like ions in the outer regions of the plasma, Peacock et al (1978). The intensity ratio for the $1s^2 - 1s2p$, $^3P_1/^1P_1$ resonance lines appears to be close to 0.7 as observed in the centre of the DITE tokamak with $n_e \simeq 2 \times 10^{13}$ cm^{-3}, Fig. 16. This value is only slightly different from the maximum theoretical stationary value predicted by Gabriel and Jordan (1972). In the cooler outer

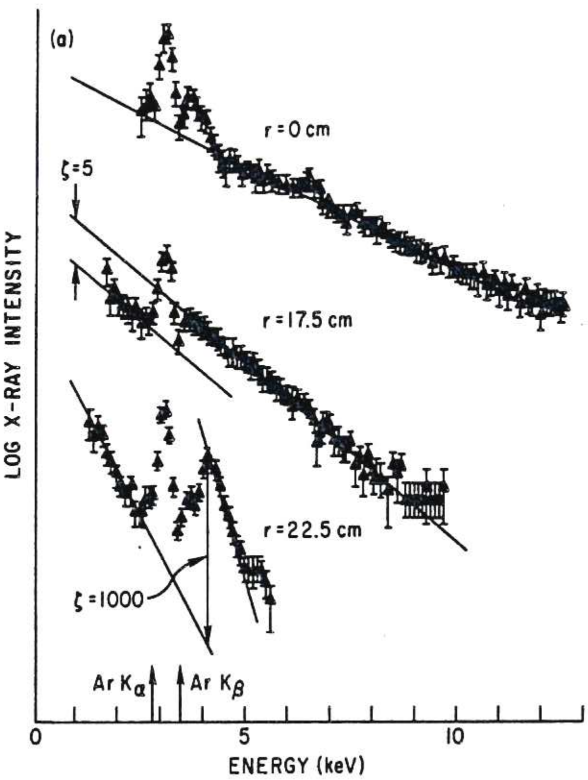

FIG.15

Continua with superimposed K_α (n = 1→2) and K_β (n = 1→3) Ar lines and Ar free-bound continuum 'steps' in the spectrum from argon-seeded PLT tokamak. The central electron temperature T_e (r=0) ∿ 1.5 keV while T_e(r=22.5) ∿ 0.5 keV; $n_e \sim 2 \times 10^{13}\ cm^{-3}$. ξ is the enhancement factor of the continuum intensity, due to recombination ($Ar^{+17} + e \rightarrow Ar^{+16}$), over the Bremsstrahlung intensity. In coronal equilibrium, ξ_{calc} << than that shown for plasma radii r ≲ 20 cm: Von Goeler (1978).

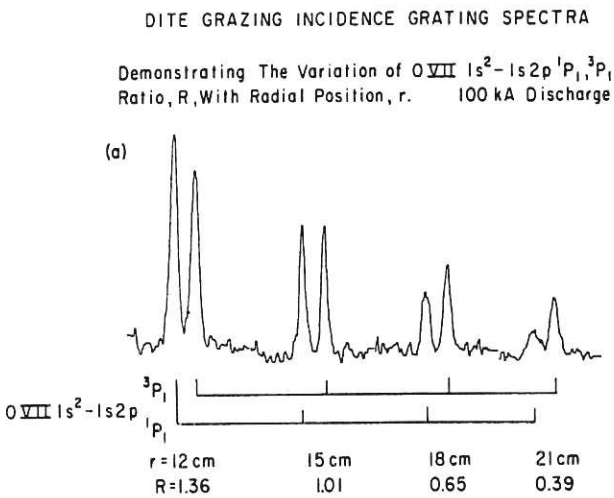

FIG.16

Intercombination and allowed lines of OVII as a function of plasma radius in the DITE tokamak. $I(2p\ ^3P_1)/(2p\ ^1P_1)$ assumes the 'stationary ratio' ≃ 0.7 in the core of the plasma but departs markedly from this value in the cool outer plasma region.

region of the plasma in DITE, the ratio exceeds 2/1 indicating much higher occupancy of the lower triplet levels than would be predicted on a stationary model, due to the effect of the recombination process, $O^{7+} + e \rightarrow O^{6+}$.

Using theoretical indicated plots of the singlet and triplet level populations for O^{6+} as a function of temperature and density, Peacock and Summers (1978), the departure of the $1s^2$-1s2p, $^3P_1/^1P_1$ resonance lines have been interpreted in terms of an outward diffusion of O^{7+} with a velocity $V_r \sim 10^2$ cm s^{-1}, Peacock et al (1978).

Both of the above spectral features, the x-ray recombination edge and the triplet/singlet ratio are very attractive from the point of view of diagnostic measurements of the 1-electron ion diffusion velocities. Essentially, the techniques depend on radial measurements of only one spectral feature (in the case of the triplet/singlet, this feature is two neighbouring lines) and no absolute instrument calibration is involved. Ordinarily in order to measure ion diffusion rates, the radial distributions of the absolute concentrations of several neighbouring ion species is required. A caveat to the use of these diagnostic techniques however is the possible inclusion of charge transfer recombination with thermal neutrals, e.g. H^o, at the edge of the plasma.

5.3 Atomic Structure of 1- and 2-Electron Systems

The energy levels of highly-ionised 1- and 2- electron ions are of fundamental interest in the theory of atomic structure. Several terms contribute to the n=2 level structure but these may be lumped into the main electrostatic potential (proportional to Z^2 for H-like ions) with fine structure, relativistic and radiative (QED) corrections, the latter three being proportional to Z^4. High Z ions are in some ways a better test of quantum electrodynamic theory (QED) than is the H atom, since the higher order radiative terms scale as Z^n. The non QED component of the energy levels $2p\ ^2P_{3/2,\ 1/2}$ and $2s\ ^2S_{1/2}$ can in principle be calculated with a precision of the order of 1 in 10^5 so that subtraction of the non QED component from precision experimental values of the energy levels should provide a good test of QED theory. Tests of the $1s_{1/2}-\ ^2P_{1/2}$ Lamb shift measurements in 1-electron ions have been reviewed by Kugel and Murnick (1977) and by Mohr (1976). For Z > 9, Lamb shifts have not been tested to an accuracy better than 1%.

The most tried method of unfolding the Lamb shift contribution has been to observe a 'quench' peak in the $2s_{1/2}$ decay spectrum produced in beam-foil experiments. Mixing of the $2s_{1/2}$, $2p_{1/2}$ levels by a velocity-induced electric field can be interpreted theoretically, a contribution to the quenching being due to the Lamb shift, Gould and Marrus (1978). Another possibility is to measure the resonance absorption of the $2s_{1/2}$ metastable level and the $2p_{1/2,\ 3/2}$ levels using tunable lasers.

The use of a tokamak plasma as a spectroscopic source for measuring the term structure of 1- and 2- electron ions is an alternative possibility. It is clearly possible as illustrated in Fig.13 to generate the appropriate highly-charged ions and using high dispersion crystal diffraction to make precision measurements on the $n=1\rightarrow 2$ lines. In order to make some impact on QED theory however, wavelength measurements of the centroid of the lines to $\sim$ 1 part in 10^6 is necessary, the Lamb shift contribution being 1 part in 2×10^4 for $Z \simeq 20$. Such high resolution spectroscopy on lines which suffer from plasma broadening (thermal and mass-motion e.g. rotation) and from radiation damping ($\Delta E = h\sum_i A_{ji}$, i.e. proportional to Z^4 for the lines in Fig.13), while not impossible, will be a 'tour de force' in tokamak spectroscopy.

It has been pointed out by several authors e.g. Ermolaev (1973), Berry et al (1978) that Lamb shift measurements need not be confined to 1-electron ions and that 2-electron ions may indeed offer higher precision. This is especially the case with the transitions 1s2s $^3S_1$ - 1s2p $^3P_{2,1,0}$. These $\Delta n=0$ lines have energies scaling as Z in contrast to the Lamb shift scaling as $(\alpha Z)^4$. The progressive increase in the energy of the Lamb shift relative to the n=2, $^3S_1$ - $^3P_{2,1,0}$ transition energy Fig.17 is such that at Z=20, the QED contribution is $\sim$ 1%, Ermolaev and Jones (1974). The wavelength of the 1s2s-1s2p triplet lies typically in the region $100Å \leq \lambda \leq 1000Å$ for Z > 10, and precision wavelengths for most of these transitions have still to be measured.

FIG.17

Lamb shift fraction of 1s2s $^3S_1$ - 1s2p $^3P_0$ energy as a function of nuclear charge.

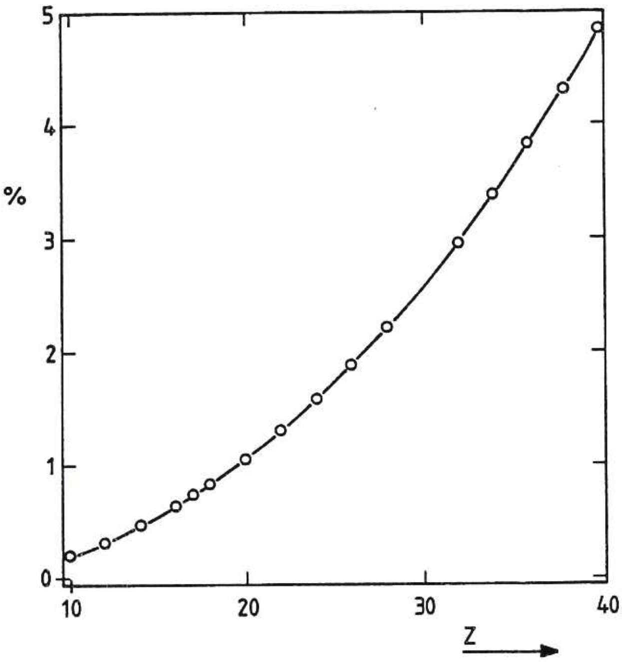

Lamb shift as a fraction of 1s 2s $^3S_1$-1s 2p $^3P_0$

Beam foil techniques have been used to measure the 1s2s $^3S_1$ - 1s2p $^3P_{2,1,0}$ transitions in Ar^{+16}, Davis and Marrus (1977), and in Si^{+12}, O'Brien et al (1979) and in Cl^{+15} Berry et al (1978). These latter authors use high quantum, i.e. almost hydrogenic transitions e.g. n=8→9 from the beam source as wavelength standards and claim about 1% precision in the Lamb shift contribution to the total transition energy. The Lamb shift is evaluated by subtracting the theoretical non QED contribution from the measured energy levels.

In 2-electron systems the ionisation potential is $I_{tot} = I_{rel} + E_1$, where I_{rel} is the electrostatic energy with relativistic corrections and E_1, proportional to $\left(\frac{\alpha^3 Z^4}{n^3}\right)$, contains both the singlet-triplet fine structure terms and the Lamb shift, i.e $E_1 = E_{st} + E_{QED}$. Ermolaev and Jones (1972) indicate that configuration mixing corrections to the fine structure splitting, $^3P_{2,1,0}$, is not important for $Z < 10$ where $E_{st} \simeq E_{QED}$ but must be included for $Z > 10$ where E_{st} exceeds E_{QED}. As Z increases spin-orbit coupling breaks down and progressive mixing of the $^1P_1$ and $^3P_1$ levels causes (E1) resonance decay of the intercombination line $1s^2\ ^1S_o - 1s2p\ ^3P_1$. The two strongest lines of the $\Delta n=0$ triplet are then $1s2s\ ^3S_1 - 1s2p\ ^3P_{2,0}$. Electron correlations are significant for the $^3P_0$ energy level, Berry et al (1978), leaving the $^3P_2$ level for QED measurements.

In tokamaks, the $1s2s\ ^3S_1 - 1s2p\ ^3P_{2,1,0}$ lines can be intense as seen with the OVII triplet emission from DITE, Fig. 9. For the OVII n=2 triplet levels, $\sim$ 1% of the energy is due to fine structure while $\sim$ 0.1% is due to the Lamb shifts. In order to measure the latter to 1 part in 100 say, a wavelength precision $\delta\lambda \simeq 0.02$Å is required. In the normal incidence region of the spectrum this wavelength accuracy is readily attainable. For higher Z ions, say z = 20, the situation is even more promising and a wavelength accuracy of 0.01Å would allow extraction of the 2-electron Lamb shift with a precision of 1 part in 10^3.

While the n=2 triplet transitions for Z > 10 have yet to be observed in tokamak plasmas there is no doubting the capability of these sources of producing 2-electron spectra with high emissivity. Precision wavelength measurements from these plasmas will constitute a most interesting test of QED for electrons in an intense Coulomb field.

6. ACKNOWLEDGEMENTS

The author would like to express his thanks to M Bitter (Princeton Plasma Physics Laboratory), J D Silver (Oxford University), H P Summers (University of Strathclyde) and K D Lawson (Royal Holloway College). Discussions with these scientists have materially helped in the preparation of this paper.

REFERENCES

Afrosimov V V, Gordeev Yu S, Zinovev A N and Korotov, (1979) JETP Lett, 28 No 8, 500-502.

Axon K B, Clark W H M, Cordey J G et al (1980) Proc. 8th Int. Conf. on Plasma Physics and Controlled Fusion Research: paper IAEA CN-38/N-4. To be published IAEA Vienna.

Behring W E, Cohen L, Feldman V and Doschek G A, (1976) Astrophys. Jnl, 203, 521-527.

Bely-Dubau F, Gabriel A H and Volonte S (1979a) Mon.Not.Roy.Astr.Soc. 186 405-419.

Bely-Dubau F, Gabriel A H and Volonte S (1979b) Ibid 189, 801-816.

Berry H G, Deserio R and Livingston A F (1978) Phys.Rev.Letts. 41 1652-1655.

Betz H D (1972) Rev.Mod.Phys. 44 465-539.

Bhalla C P, Gabriel A H, Presnyakov L P (1975) Mon.Not.Roy.Astron.Soc. 172 359-375.

Bhatia A K and Mason H E (1980) Astron. Astrophys. 83 380-382.

Bitter M, Hill K W, Sautoff N R, Efthimion P C Meservey E, Roney W, Von Goeler S, Horton R, Goldman M and Stodiek W (1979) Phys.Rev.Lett. 43 No.2 129-132.

Bitter M Von Goeler S, Horton R, Goldman M, Hill K W, Sauthoff N R and Stodiek W (1979) Phys.Rev.Lett. 42 No.5 304-307.

Bohr N and Lindhard J (1954) Kgl.Danske Videnskab. Selsk, Mat.Fys.Medd. 28 No.7.

Brau K, Von Goeler S, Bitter M, Cowan R D, Eames D, Hill K, Sauthoff N, Silver E Stodiek W (1980) Princeton Plasma Physics Laboratory Report PPPL-1644.

Bransden B H (1972) Rep.Prof.Phys. 35 949-1005.

Breton C, De Michelis C, Finkenthal M and Matticli M (1978) Phys.Rev.Letts 41 No 2 110-113.

Burgess A (1965) Astrophys. Jnl. 141 1588-1590.

Cowan R S, "Spectra of Highly-Ionised Atoms of Tokamak Interest" (1977) Los Alamos Laboratory Report LA-6679-MS.

Crandall D H (1979) Invited paper at Int. Seminar on Ion-atom Collisions (ISIAC VI) at JAERI Tokai-Mura Japan 1979.

Davis W A and Marrus R (1977) Phys.Rev. 15A 1963-1975

Doschek G A and Feldman U, (1976) Jnl.Appl.Phys. 47 3083-3087.

Doschek G A, Feldman U, Dere K P, Sandlin G D, Van Hoosier M E, Brueckner G E, Purcell J D and Tousey (1975) Astrophys. Jnl. 196, L83-86.

Edlén B (1969) Solar Physics 9, 439-445.

Edlén B (1972) Solar Physics 24, 356-367

Edlén B (1979a) Physica Scripta, 19, 255-266.

Edlén B (1979b) Physica Scripta, 20, 129-137.

Edlén B (1980) to be published in Physica Scripta

Edlén B (1945) Mon.Not.Roy.Astro.Soc. 105 323-333.

Ermolaev A M (1973) Phys.Rev. A 8 No.3 1651-1657.

Ermolaev A M and Jones M (1974) J.Phys.B.Atom Molec.Phys. 7 No.2 199-207.

Ermolaev A M and Jones M (1972) J.Phys.B.Atom Molec.Phys. 5 L225-228.

Eubank H, Goldston R J et al (1979) Nuclear Fusion Suppl. 1 167-197, publ. by IAEA Vienna.

Fawcett B C (1975), Atomic Data and Nuclear Data Tables 16 135-164.

Fawcett B C (1978), Atomic Data and Nuclear Data Tables, 22 473-489.

Feldman U, Doschek G A, Chung-Chieh Cheng and Bhatia A K, (1980) J.Appl.Phys. 51 (1) 190-201.

Freeman F F, Gabriel A H, Jones B B and Jordan C (1971) Phil.Trans.Roy.Soc. (London) A 270 127- 133.

Gabriel A H, Mon.Not.Roy.Astron.Soc. (1972) 160, 99-199.

Gabriel A H and Jordan C (1972) Case Studies on Atomic Collision Physics, Vol 2 Chap 4, publ. North Holland (1972).

Gabriel A H and Phillips K J H (1980) Mon.Not.Roy.Astr.Soc. to be publ.

Gorzdanov T P and Janev R K (1978), Phys.Rev.A 17 880-896.

Gould H and Marrus R (1978) Phys.Rev.Letts. 41 No.21, 1457-1460.

Hugill J, Fielding S J et al (1977) Proc. 8th Euro.Conf. on Controlled Fusion and Plasma Physics (Prague 1977) publ. as Culham Laboratory Preprint (1977) CLM-P492 paper 1.

Hulse R A, Post D E, Mikkelsen D M (1980) Princeton Plasma Physics Laboratory Report PPPL-1633.

Isler R C (1977) Phys.Rev.Lett 38 1359-1362.

Isler R C and Crume E C (1978) Phys.Rev.Lett. 41 1296-1300.

Jenson R V, Post D E, Grasberger W H, Tarter C B and Lokke W A (1977) Nucl. Fus. 17 1187-1196.

Krupin V A, Marchenko V S and Yakovlenko S I (1979) JETP lett. 29 No.6 318-321.

Kugel H W and Murnick D E (1977) Rep.Prog.Phys. 40, 297

Lawson K D and Peacock N J (1980) J.Phys.B. Atom.Molec.Phys. to be publ.

Lawson K D, Peacock N J and Stamp M F (1980) J.Phys.B. Atom.Molec.Phys. to be publ.

Lotz W, (1967) Astrophys.J.Suppl. 14, 207-238.

Loulergue M and Nussbaumer H (1973) Astron.Astrophys. 24 209-213.

Mansfield M W D, Peacock N J, Smith C C, Hobby M G, Cowan R D (1978) J.Phys.B. Atom.Molec.Phys. 11, 9, 1521-1544.

Mason H E, Doschek G A, Feldman U and Bhatia A K,(1979) Astron.Astrophys. 73 74-81.

Merts A L, Cowan R D, Magee N H, "The Calculated Power Output from a Thin Ion-seeded Plasma" (1976) Los Alamos Report LA-6220MS.

Mohr P J (1976) in "Beam Foil Spectroscopy' Vol 1, edited by I A Sellin and D J Pegg (Plenum, NY) 89.

O'Brien R, Silver J D, Jelley N A, Bashkin S, Trabert E and Heckmann P H (1979) J.Phys.B, Atom.Molec.Phys. 12 No.2 L41-44.

Olson R E and Salop A (1977) Phys.Rev.A 16 531-541.

Olson R E and Salop A (1976) Phys.Rev.A 14 579-585.

Peacock N J, Hughes M H, Summers H P, Hobby M G, Mansfield M W D and Fielding S J (1979), Plasma Physics and Controlled Fusion Research (Innsbruck, 1978) Nuclear Fusion Supplement, Publ. IAEA Vienna, Vol.1 303-314.

Peacock N J and Summers H P (1978), J.Phys.B. Atom.Molec.Phys. 11 No.21 3757-3774.

Post D E, Jensen R V, Tarter C B, Grasberger W H and Lokke W A (1977) Atomic Data and Nuclear Tables 20, 397-439.

Ryufuku H and Watanabe T, (1978) Phys.Rev.A 18 2005-2015
(1979a) Ibid 19 1538
(1979b) Ibid 20 1828

Samain A and Werkoff F (1977) Nuclear Fusion 17, 1 53-64

Stringer T E (1977) Proc. of Course "Theory of Magnetically Confined Plasmas" Varenna 1977. Publ. by Pergamon Press for Commission of the European Communities.

Suckewer S and Eubank H P, Goldston R J, Hinnov E and Sauthoff N R (1979) Phys.Rev.Lett. 43 207-10.

Suckewer S,Fonck R and Hinnov E (1980) Phys.Rev.A 21 924-927

Suckewer S and Hinnov E (1978) Phys.Rev.Letts. 41 No.11 756-759.

Suckewer S, Hinnov E, Bitter M, Hulse R and Post D, (1980) Princeton Plasma Physics Laboratory Report PPPL-1636.

Summers H P (1974) Appleton Laboratory Report AL-R-5 publ. by SRC Rutherford-Appleton Laboratory, UK.

Summers H P and McWhirter R W P (1979) J.Phys.B 12 No.14 2387-2412.

Von Goeler S "Diagnostics for Fusion Experiments" (1978) Proc. of the Course held by the Int. School of Plasma Physics in Varenna, Italy, publ. 1979 by Pergamon Press, editors E Sindoni and C Wharton, 79-109.

Wiese W L (1978) 'Physics of Ionised Gases' 661-696, publ. Institute of Physics Belgrade.